る[6,7]．$GABA_A$受容体は神経細胞体から樹状突起に，$GABA_B$受容体は神経終末に発現している(図4)．ACh遊離に対して，$GABA_A$受容体は促進的に，$GABA_B$受容体は抑制的に働くことが，摘出臓器を用いた著者らの研究などからわかってきている[6]．

実際のGABAの作用について，麻酔をしたイヌの小腸の動きを直接測定することにより検討を行ったところ，$GABA_A$アゴニストによる腸管運動の亢進ならびにACh遊離の増加，$GABA_B$アゴニストによる腸管運動の抑制ならびにACh遊離の低下がみられた[8]．同実験においてGABAを投与すると，ACh遊離ならびに腸管運動の抑制がみられた[8]．このことはGABAの作用においては$GABA_B$受容体が優位に働いていることを示唆する(図4)．$GABA_B$受容体は中枢神経系にも広範に発現しているが，著者らはある種の$GABA_B$受容体サブタイプが特異的に消化管で発現していることを見出した．この$GABA_B$受容体に特異的な薬物を開発することであらたな消化管特異的$GABA_B$作動薬を開発できる可能性がある[9]．

おわりに

消化管神経叢の消化管運動における重要な役割について，また腸管神経叢に発現している種々の受容体に作用する薬物が消化管機能調整薬として用いられていることを概説した．腸管神経叢の解剖学的構造ならびに神経叢に発現している種々の受容体の薬理学的性質を理解したうえで消化管作動薬の働きを考えると，その作用を理解しやすいことがわかる．また，末梢のオピオイド受容体のみを抑制するオピオイド依存性便秘の改善薬や，$GABA_B$受容体作動薬の臨床開発など，腸管神経叢に存在する受容体に作用するあらたな薬物の開発・上市にも注目したい．

文献

1) Alexander, S. P. H. et al.：*Br. J. Pharmacol.*, **158** (Suppl. 1)：S1-S254, 2009.
2) Nakayama, S. et al.：*J. Pharmacol. Exp. Ther.*, **254**：792-798, 1990.
3) Taniyama, K. et al.：*Gastroenterology*, **101**：1579-1587, 1991.
4) Thomas, J. et al.：*N. Engl. J. Med.*, **358**：2332-2343, 2008.
5) Shichijo, K. et al.：*Am. J. Physiol.*, **273**：G1044-G1050, 1997.
6) Tanaka, C. and Taniyama, K.：The role of GABA in the peripheral nervous system. *In*：GABA outside the CNS (ed. by Erdo, S. L. and Bowery, N. G.). Springer-Verlag, Berlin, 1991, pp.3-17.
7) Uezono, Y. et al.：*J. Pharmacol. Sci.*, **94**：211-213, 2004.
8) Kawakami, S. et al.：*J. Pharmacol. Sci.*, **94**：368-375, 2004.
9) Torashima, Y. et al.：*J. Pharmcol. Sci.*, **111**：253-259, 2009.

* * *

パクリタキセル誘発性末梢神経障害のメカニズム

宮野加奈子[1)]
上園保仁[1)]　仲田義啓[2)]
[1)]国立がん研究センター研究所がん患者病態生理研究分野
[2)]広島大学大学院医歯薬学総合研究科薬効解析科学

要　旨
パクリタキセルは，乳がんなどの化学療法に用いられるが，末梢神経障害を引き起こす．中でも，痛みに対して効果的な予防や軽減の方法が確立されていない．そのため，その重篤さから化学療法を中止せざるを得ないことがあり，有益ながん治療を受けることが困難になる場合すらある．パクリタキセル治療による末梢神経障害発生メカニズムを明らかにし，その対策を確立することはがん患者の quality of life（QOL）の向上に極めて重要である．今回はパクリタキセル誘発性末梢神経障害のメカニズムの一端を紹介する．

（ペインクリニック 32：1491-1498，2011）
キーワード：パクリタキセル，末梢神経障害，サブスタンス P

はじめに

パクリタキセルは，太平洋イチイ（*taxus brevifolia*）から単離された薬物である．この薬物は，チュブリンの重合により構成されている微小管に作用し，細胞分裂に必要な紡錘体の正常な形成を阻害する結果，がん細胞などの増殖を抑制する．現在，パクリタキセルは卵巣がんや乳がんをはじめ様々な固形がんの化学療法に用いられる優れた抗がん剤である．しかし，その一方で様々な副作用を引き起こすことが知られている．中でも末梢神経障害は，がん患者にとって重篤な副作用の一つであり，末梢神経（感覚神経，運動神経，自律神経）のうち感覚神経が障害されやすい[1,2)]．そのため，パクリタキセル投与 24～72 時間後から，感覚異常，知覚麻痺，刺痛，灼熱痛，ならびに機械刺激や冷刺激などに対するアロディニアが現れ始める[2)]．これらの症状は四肢末端から生じ，一般的には可逆的であるが，回復するまでには時間がかかることが多く，不可逆的になる場合もある．実際に，パクリタキセルによる化学療法を受けたがん患者の 59～78％に末梢神経障害が認められ[2)]，そのうちの約 30％は日常生活に支障をきたすことが報告されている[3)]．そのため，パクリタキセル投与による末梢神経障害は，がん患者の QOL に大いに影響を与える．しかしながら，パクリタキセルによる末梢神経障害発生メカニズムについては現段階で不明な点が多く，効果的な予防法や症状軽減の方法は確立されていない．パクリタキセル治療を受けているがん患者の中には，しばしばその重篤さから化学療法の変更あるいは中止を余儀なくされることがあり，有益ながん治療の継続が困難になることがある．これらのことから，パクリタキセ

〈Special Article〉 Essentials of neuropathic pain which support clinical data
The mechanism of paclitaxel-induced peripheral neuropathy
Kanako Miyano, et al
Division of Cancer Center Pathophysiology, National Cancer Center Research Institute

ル治療による末梢神経障害の発生メカニズムを明らかにし，その予防や軽減の方法を開発することは非常に重要である．

本稿では，パクリタキセルの末梢神経障害発生メカニズムについて，これまでの知見，ならびに筆者らの行った研究から得られた成果を紹介する．

1．パクリタキセルは一次感覚神経に蓄積する

パクリタキセルによる神経障害は，中枢神経より末梢神経に発生しやすいことが知られている[1,2]．実際，パクリタキセルは血液－脳関門（blood-brain barrier）を通過しにくく，血漿中のパクリタキセル量は脳脊髄液中の約500倍にも及ぶ[4]．また，パクリタキセルは，一次感覚神経の細胞体が存在する脊髄後根神経節（dorsal root ganglia：DRG）と末梢神経に蓄積しやすい[5]．血漿中のパクリタキセル量と比較し，DRGでは約200倍，末梢神経では約20倍の量のパクリタキセルが蓄積することが報告されている[5]．パクリタキセル治療による末梢神経障害の発生メカニズムの詳細は今のところ明らかにされていないが，少なくともパクリタキセルは，DRGと末梢神経，中でも一次感覚神経に作用することにより末梢神経障害を発生する可能性が考えられる．

2．パクリタキセルによる末梢神経障害の発生メカニズム

1）一次感覚神経における病態生理

一次感覚神経は，Aβ，Aδ，C線維の3つに大別される．Aβ線維は太い有髄線維であり，触覚や圧覚などの非侵害性刺激情報を伝達する．一方，Aδ線維は有髄，C線維は細い無髄の線維であり，ともに侵害性疼痛を伝達する．前者は刺された時に感じるような即時性の痛みを，後者は灼けつくような鈍い痛みを伝達する．パクリタキセル投与による末梢神経障害モデル動物の病態時では，AβとAδ線維の軸索変性およびシュワン細胞の形態学的変化が観察される[6]．加えて，神経線維には脱髄が生じることも認められており，これが神経伝導速度の低下の要因の一つと考えられている[6]．上記のAβ，Aδ線維に認められる病態変化は，パクリタキセルが軸索の微小管を凝集させることにより生じることが示唆されている[1]．一方，C線維では，パクリタキセルがミトコンドリアに直接作用し，脱分極と異所性発火を誘導することが報告されている[7,8]．しかし，C線維については知見が少なく不明な点が多い．

2）パクリタキセルは一次感覚神経から痛覚伝達物質サブスタンスPを遊離させる

サブスタンスP（substance P：SP）は，ニューロキニン類（neurokinin：NK）に属する神経ペプチドの一つである．SPは，一次感覚神経のうちC線維に多く発現しており，熱，酸，機械刺激などの様々な侵害刺激により遊離される．C線維から遊離されたSPは，脊髄後角の二次感覚神経に発現するSP受容体（NK受容体）を活性化し，痛みを中枢へ伝達する．さらに，SPは神経障害性疼痛の形成にも重要な役割を果たしており，パクリタキセル投与によるアロディニアの発症に関与することが，最近，明らかとなった[9]．また，がん患者の血漿中SP量がパクリタキセル投与後30分で増加することも報告されている[10]．これらの事実は，C線維から遊離させるSPがパクリタキセル投与による末梢神経障害に重要な役割を果たす可能性を示唆する．そこで，まず筆者らは，ラットDRG初代培養細胞を作製し，ラジオイムノアッセイを用いてパクリタキセル処置によるSP遊離量を測定した．化学療法時の血漿中パクリタキセル濃度は最大で約10 μMとなるため[11]，測定濃度は0.1～10 μMに設定した．そ

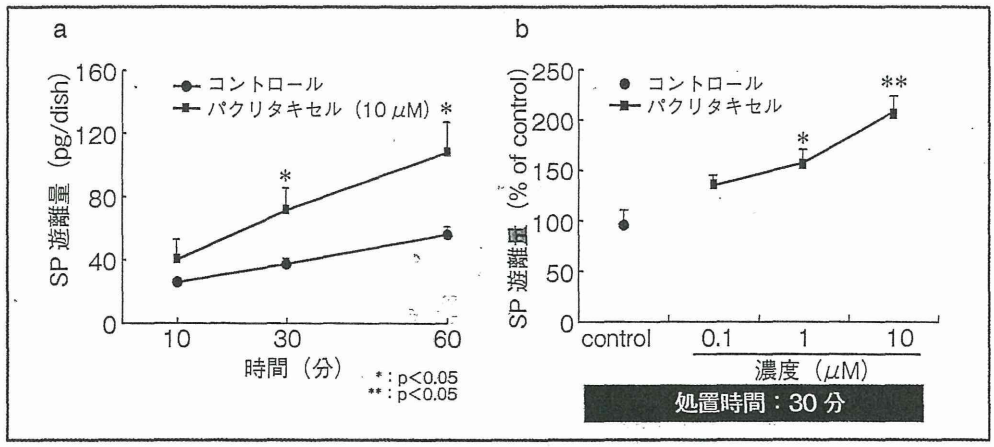

図1　パクリタキセルによる SP 遊離量の変化（文献 12 より引用改変）

の結果，パクリタキセルはラット DRG 細胞から SP を時間・濃度依存的に遊離させることが明らかとなった（図1）．したがって，パクリタキセルを用いたがんの化学療法時には，一次感覚神経から SP が遊離されている可能性が考えられる．

3．パクリタキセルによる SP 遊離機構

1）パクリタキセルはプロテインキナーゼ C 活性を介して SP を遊離させる

プロテインキナーゼ C（protein kinase C：PKC）は，制御領域の違いにより，在来型 PKC（conventional PKC：cPKC），新型 PKC（novel PKC：nPKC）および非典型 PKC（atypical PKC：aPKC）の3つに大別される．筆者らは，これまでに，DRG 細胞からの SP 遊離に cPKC および nPKC が関与することを報告している[13,14]．そこで，パクリタキセル処置による SP 遊離に対する各種 PKC 阻害薬の効果について検討した．パクリタキセル処置による SP 遊離量の増加が，cPKC および nPKC 阻害薬ビスインドールマレイミド（bisindolylmaleimide：BIM，10 μM）および cPKC 阻害薬 Gö 6976（1 μM）

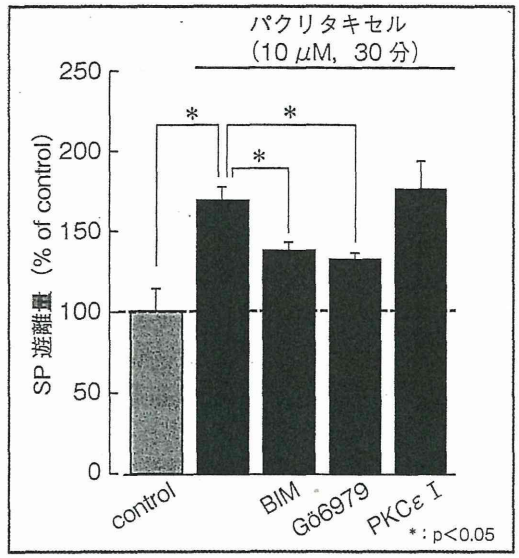

図2　パクリタキセル処置による SP 遊離に対する PKC 阻害薬の効果（文献 12 より引用改変）

の前処置（15 分間）により抑制され，その抑制効果は同等であった（図2）．

また，筆者らは，nPKC のうち PKCε サブタイプが DRG 細胞からの SP 遊離に関与していることを明らかにしている[13,14]．しかし，PKCε 阻害薬 PKCε translocation inhibitor pep-

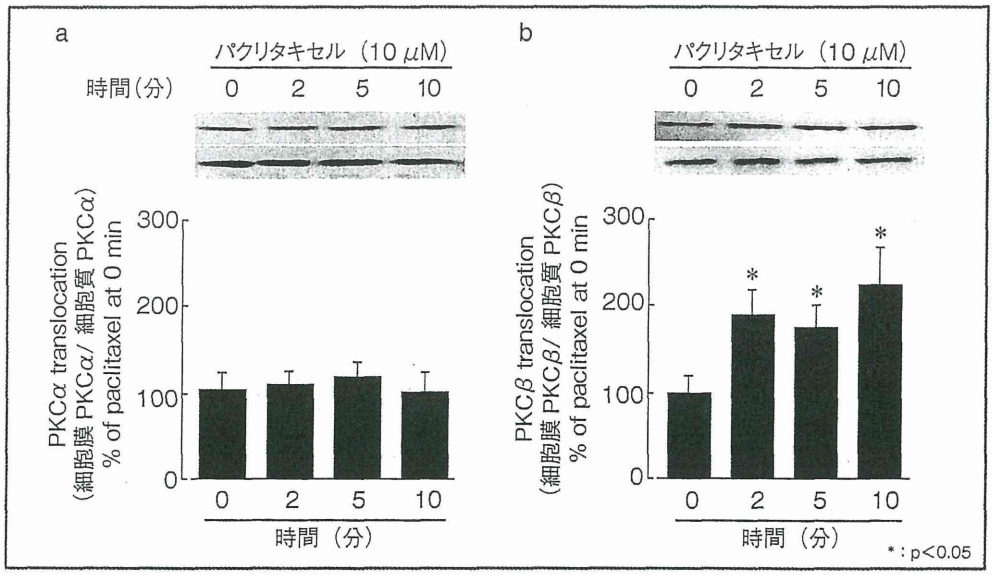

図3　パクリタキセル処置によるcPKCの細胞質から細胞膜へのトランスロケーション
（文献12より引用改変）

tide（PKCε I, 200 μM）は，パクリタキセル処置によるSP遊離量の増加に影響を及ぼさなかった（図2）．以上の結果より，cPKCがパクリタキセル処置によるSP遊離に重要であることが示唆された．

cPKCは，PKCα，βおよびγの3つのサブタイプに分類され，活性化されると細胞質から細胞膜へトランスロケートされる．ラットDRG細胞には，PKCαおよびβが発現しているので，パクリタキセル処置によるPKCαおよびβの細胞膜へのトランスロケーションをウェスタンブロッティングにより検討した．その結果，PKCαの有意なトランスロケーションは認められなかったが（図3a），PKCβの持続的なトランスロケーションが観察された（図3b）．この結果は，PKCβの活性化がパクリタキセル処置によるSP遊離に関与することを示唆している．パクリタキセルがPKCβを活性化するメカニズムについては，今後の検討が必要である．

2）パクリタキセルはtransient receptor potential（TRP）チャネルファミリーを介してSPを遊離させる

筆者らは，transient receptor potential（TRP）チャネルの活性化による細胞内へのCa^{2+}流入を介してDRG細胞からSPが遊離されることを報告してきた[14,15]．そこで，まずパクリタキセル処置によるSP遊離量増加に及ぼす細胞外Ca^{2+}の影響について検討した．パクリタキセル処置によるSP遊離量の増加は，細胞外Ca^{2+}の除去によりほぼ完全に抑制された（図4a）．また，この増加は，細胞外Ca^{2+}の細胞内への流入を阻害する$LaCl_3$存在下（300 μM）においてもほぼ完全に抑制された（図4a）．これらのことから，パクリタキセル処置によるSP遊離に，細胞外から細胞内へのCa^{2+}流入が不可欠であることが明らかとなった．

次に，パクリタキセル処置で起こるSP遊離量の増加に対する各種TRPチャネル阻害薬の効果を検討した．パクリタキセル処置による

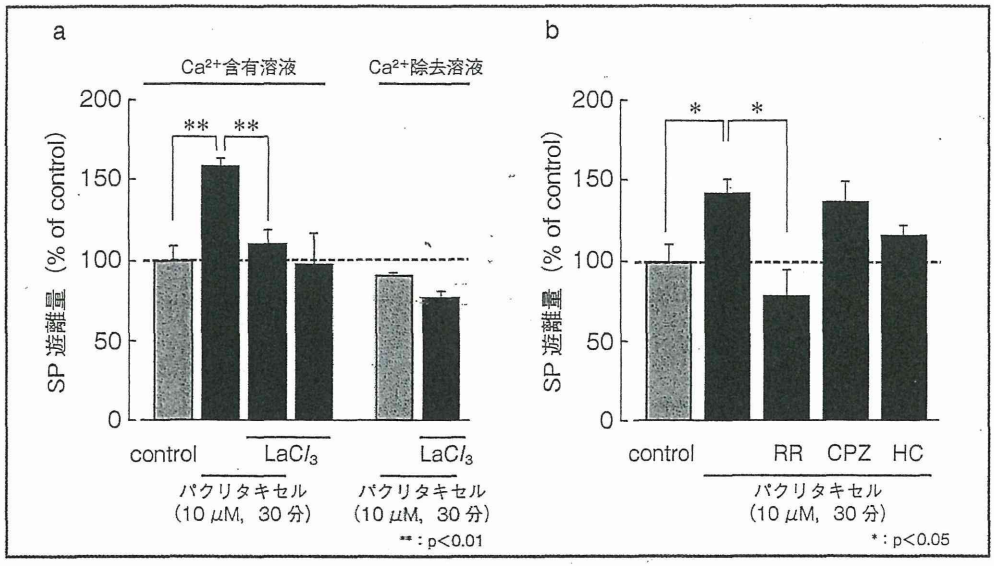

図4　パクリタキセル処置によるSP遊離に及ぼす細胞外Ca^{2+}ならびにTRPチャネル阻害薬の影響（文献12より引用改変）

SP遊離量の増加は，TRPチャネル阻害薬ルテニウムレッド（ruthenium red：RR，50 μM，15分間）前処置により有意に抑制された（図4b）．筆者らは，TRPチャネルサブファミリーのうちTRPV1（transient receptor potential vanilloid 1）がDRG細胞からのSP遊離を調節していることを報告している[14,15]．また，DRGにおいて，TRPV1はTRPA1（transient receptor potential ankyrin 1）と共発現しており[16,17]，TRPA1はTRPV1と類似した作用を有する可能性が示唆されている[18,19]．そこで，TRPV1およびTRPA1が，パクリタキセル処置によるSP遊離を制御するTRPチャネルの候補の一つとして考えられた．しかし，TRPV1阻害薬カプサゼピン（capsazepine：CPZ，1 μM）およびTRPA1阻害薬HC-030031（HC，10 μM）では有意な抑制効果は認められなかったことから（図4b），この遊離にはTRPV1およびTRPA1以外のTRPチャネルが関与している可能性が考えられた．TRPV1およびTRPA1以外のルテニウムレッド感受性のTRPチャネルとしては，TRPV3，TRPV4などがあり[20]，これらのチャネルはSP含有DRG細胞と共発現している[21]．以上の結果を統合すると，パクリタキセルはTRPV1およびTRPA1以外のルテニウムレッド感受性TRPチャネルを介してSPを遊離させることが考えられる．どのようなTRPチャネルのサブタイプがパクリタキセル処置によるSP遊離に関与するかについては，今後の検討を要する．

上述した結果より，パクリタキセルによるSP遊離に，TRPチャネルを介した細胞外から細胞内へのCa^{2+}の流入が関与することが示唆された．そこで，ラットDRG細胞におけるパクリタキセル処置による細胞内Ca^{2+}濃度変化をCa^{2+}イメージングアッセイにより測定した．その結果，パクリタキセル処置（10 μM）数分後から持続的な細胞内Ca^{2+}濃度の上昇が観察された（図5a）．また，この上昇は，細胞外Ca^{2+}の除去，ならびにルテニウムレッドの前処置によりほぼ完全に抑制された（図5b，c）．これらの結果より，パクリタキセルはTRP

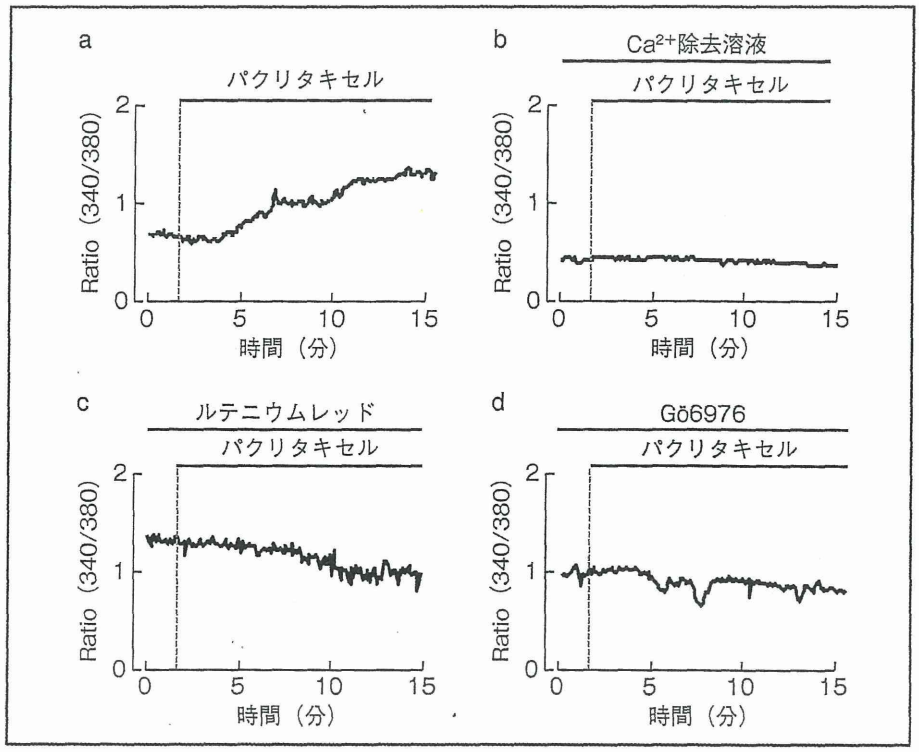

図5　パクリタキセル処置による細胞内 Ca^{2+} 濃度変化（文献 12 より引用改変）

チャネルを介して細胞外からの Ca^{2+} 流入を引き起こすことが示唆された．さらに，パクリタキセル処置による細胞内 Ca^{2+} 濃度の上昇は，Gö6976 によりほぼ完全に抑制されたことから（図5d），パクリタキセルは，まず PKCβ を活性化させ，その結果，細胞外から細胞内へ Ca^{2+} 流入が起こり，SP を遊離させることが示唆された．近年，PKC は温度感受性 TRP チャネルをリン酸化することにより温度閾値を低下させ，TRP チャネルを開口させる可能性が示されている[20,22,23]．したがって，パクリタキセルは，PKCβ による TRP チャネルのリン酸化を介してチャネルを開口させる可能性が考えられる．しかし，パクリタキセルにより活性化された PKCβ が TRP チャネルを実際にリン酸化するのかについては，今後の検討を待たなければならない．

おわりに

パクリタキセルによる末梢神経障害は，一次感覚神経の Aβ，Aδ 線維の脱髄などを引き起こすことにより生じると考えられてきたが，C 線維から遊離される SP もその成因に関与することが，近年の研究により明らかとなってきた．筆者らは，パクリタキセルによる一次感覚神経からの SP 遊離機構を明らかにし，パクリタキセルが PKCβ 活性化を介した TRP チャネルの開口により，SP を遊離させることを示した（図6）．また，近年の報告では，パクリタキセルの末梢神経障害にマクロファージ，脊髄ミクログリアおよびアストロサイトなども関与するこ

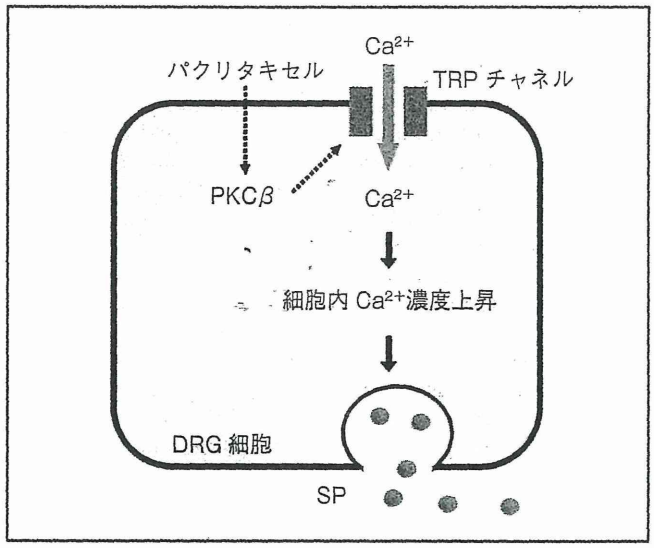

図6　DRG 細胞におけるパクリタキセルによる SP 遊離機構

とが示唆されている[24]．これらの知見を統合すると，今後はパクリタキセル投与による末梢神経障害の発生メカニズムの解明には，感覚神経だけでなく非神経細胞の関与も考慮に入れて検討する必要があるだろう．

文　献

1) Balayssac D, Ferrier J, Descoeur J, et al: Chemotherapy-induced peripheral neuropathies: From clinical relevance to preclinical evidence. Expert Opin Drug Saf 10 : 407-417, 2011
2) Roeinsky EK, Chaudhry V, Cornblath DR, et al: Neurotoxicity of taxol. J Natl Cancer Inst Monogr 15 : 107-115, 1993
3) Lee JJ, Swain SM: Pheripherial neuropathy induced by microtubule-stabilizing agents. J Clin Oncol 24 : 1633-1642, 2006
4) Glants MJ, Choy H, Kearns CM, et al: Paclitaxel disposition in plasma and central nervous systems of human and rats with brain tumors. J Natl Cancer Inst 87 : 1077-1081, 1995
5) Cavaletti G, Cavalletti E, Oggioni N, et al: Distribution of paclitaxel within the nervous system of the rat after repeated intravenous administration. Neurotoxicology 21 : 389-393, 2000
6) Authier N, Gillet JP, Fialip J, et al: Description of a short-term taxol-induced nociceptive neuropathy in rats. Brain Res 887 : 239-249, 2000
7) Flatters SJ, Bennett GJ: Studies of peripheral sensory nerves in paclitaxel-induced painful peripheral neuropathy: Evidence for mitochondrial dysfunction. Pain 122 : 245-257, 2006
8) Jin HW, Flatters SJ, Xiao WH, et al: Prevention of paclitaxel-evoked painful peripheral neuropathy by acetyl-*L*-carnitine: Effects on axonal mitochondria, sensory nerve fiber terminal arbors, and cutaneous Langerhans cells. Exp Neurol 210 : 229-237, 2008
9) Tatsushima Y, Egashira N, Kawashiri T, et al: Involvement of substance P in peripheral neuropathy induced by paclitaxel but not oxaliplatin. J Pharmacol Exp Ther 337 : 226-235, 2011
10) Sendo T, Itoh Y, Goromaru T, et al: Role of substance P in hypersensitivity reactions induced by paclitaxel, an anticancer agent. Peptides 25 : 1205-1208, 2004
11) Tamura T, Sasaki Y, Nishiwaki Y, et al: Phase I study of paclitaxel by three-hour infusion: Hypotension just after infusion is one of the major dose-limiting toxicities. Jpn J Can-

cer Res 86 : 1203-1209, 1995
12) Miyano K, Tang HB, Nakamura Y, et al : Paclitaxel and vinorelbine, evoked the release of substance P from cultured rat dorsal root ganglion cells through different PKC isoform-sensitive ion channels. Neuropharmacology 57 : 25-32, 2009
13) Tang HB, Li YS, Arihiro K, et al : Activation of the neurokinin-1 receptor by substance P triggers the release of substance P from cultured adult rat dorsal root ganglion neurons. Mol Pain 3 : 42, 2007
14) Tang HB, Li YS, Miyano K, et al : Phosphorylation of TRPV1 by neurokinin-1 receptor agonist exaggerates the capsaicin-mediated substance P release from cultured rat dorsal root ganglion neurons. Neuropharmacology 55 : 1405-1411, 2008
15) Tang HB, Nakata Y : The activation of transient receptor potential vanilloid receptor subtype 1 by capsaicin without extracellular Ca^{2+} is involved in the mechanism of distinct substance P release in cultured rat dorsal root ganglion neurons. Naunyn Schmiedeberg's Arch Pharmacol 377 : 325-332, 2008
16) Kondo T, Obata K, Miyoshi K, et al : Transient receptor potential A1 mediates gastric distention-induced visceral pain in rats. Gut 58 : 1342-1352, 2009
17) Salas MM, Hargreaves KM, Akopian AN : TRPA1-madiated responses in trigeminal sensory neurons : Interaction between TRPA1 and TRPV1. Eur J Neurosci 29 : 1568-1578, 2009
18) Bautista DM, Jordt SE, Nikai T, et al : TRPA1 mediates the inflammatory actions of environmental irritants and proalgesic agents. Cell 124 : 1269-1282, 2006
19) Nilius B : TRP channels in disease. Biochim Biophys Acta 1772 : 805-812, 2007
20) Patapoutian A, Peier AM, Story GM, et al : ThermoTRP channels and beyond : Mechanisms of temperature sensation. Nat Rev Nurosci 4 : 529-539, 2003
21) Facer P, Casula MA, Smith GD, et al : Differential expression of the capsaicin receptor TRPV1 and related novel receptors TRPV3, TRPV4 and TRPM8 in normal human tissues and changes in traumatic and diabetic neuropathy. BMC Neurol 7 : 11, 2007
22) Venkatachalam K, Montell C : TRP channels. Annu Rev Biochem 76 : 387-417, 2007
23) Grant AD, Cottrell GS, Amadesi S, et al : Protease-activated receptor 2 sensitizes the transient receptor potential vanilloid 4 ion channel to cause mechanical hyperalgesia in mice. J Physiol 578 : 715-733, 2007
24) Peters CM, Jimenez-Andrade JM, Kuskowski MA, et al : An evolving cellular pathology occurs in dorsal root ganglia, peripheral nerve and spinal cord following intravenous administration of paclitaxel in the rat. Brain Res 1168 : 46-59, 2007

※　　※　　※

SYNAPSE 66:747–751 (2012)

Short Communication

Changes in the Melanocortin Receptors in the Hypothalamus of a Rat Model of Cancer Cachexia

MASAMI SUZUKI,[1] MINORU NARITA,[2] MAHO ASHIKAWA,[3] SADAYOSHI FURUTA,[3] MOTOHIRO MATOBA,[4] HIROKI SASAKI,[5] KAZUYOSHI YANAGIHARA,[6] KIYOSHI TERAWAKI,[1] TSUTOMU SUZUKI,[3] AND YASUHITO UEZONO[1]*

[1]*Division of Cancer Pathophysiology, National Cancer Center Research Institute, 5-1-1 Tsukiji, Chuo-ku, Tokyo 104-0045, Japan*

[2]*Department of Pharmacology, Hoshi University School of Pharmacy and Pharmaceutical Sciences, 2-4-41 Ebara, Shinagawa-ku, Tokyo 142-8501, Japan*

[3]*Department of Toxicology, Hoshi University School of Pharmacy and Pharmaceutical Sciences, 2-4-41 Ebara, Shinagawa-ku, Tokyo 142-8501, Japan*

[4]*Division of Palliative Medicine and Psycho-Oncology Palliative Care Team, National Cancer Center, 5-1-1 Tsukiji, Chuo-ku, Tokyo 104-0045, Japan*

[5]*Division of Genetics, National Cancer Center Research Institute, 5-1-1 Tsukiji, Chuo-ku, Tokyo 104-0045, Japan*

[6]*Laboratory of Molecular Cell Biology, Department of Life Sciences, Yasuda Woman's University Faculty of Pharmacy, 13-1 Yasuhigashi 6-chome, Asaminami-ku, Hiroshima 731-0153, Japan*

KEY WORDS stage-dependent cancer cachexia; central melanocortin system; hypothalamus; rat

Cancer cachexia affects up to 80% of patients with advanced cancers and accounts for nearly 30% of cancer-related deaths (Acharyya et al., 2005; Fearon, 2008; Tisdale, 2009). The close association between chronic illness such as cancer and the deterioration of nutritional status not only impairs the quality of life but also increases the risk for morbidity and mortality (Norman et al., 2008). Cancer cachexia syndrome is characterized by anorexia and a loss of body weight associated with reduced muscle mass and adipose tissue. In addition to a variable contribution from decreased energy intake, the resting energy expenditure can be elevated in cancer cachexia. It is well known that advanced stages of cancer are scarcely responsive to available pharmacological and nutritional treatments, which suggests that, once a critical point is reached, it may be difficult to improve the metabolism and the availability of nutrients. Accordingly, clinicians require more effective treatments.

Recently, cachexia and precachexia were defined by the Special Interest Group on cachexia–anorexia in chronic wasting diseases. This group advocates the new concept that the mechanisms that ultimately lead to severe wasting in cachexia, that is, late-stage cachexia, are occurring early during the natural history of the disease, which suggests that appropriate interventions in early-stage cachexia might be effective for preventing the onset of this syndrome (Muscaritoli et al., 2010). This underscores the need for appropriate pharmacological and nutritional interventions to prevent precachexia from progressing to cachexia.

The central melanocortin system directly controls nutrient intake and energy metabolism (Garfield et al., 2009). Melanocortins (α-, β-, and γ-melanocyte-stimulating hormones and adrenocorticotropic hormone) are peptides derived from the proteolytic cleavage of pro-opiomelanocortin (POMC). Five melanocortin receptor (MC1R–MC5R) subtypes mediate the diverse actions of these melanocortins. Of these five MCRs, MC3R and MC4R are predominantly expressed in the brain and are involved in regulating energy homeostasis. Extensive localization studies have shown that MC3R and MC4R are highly expressed in the paraventricular nucleus (PVN), including both parvicellular and magnocellular neurons, of the hypothalamus. The activation of MC4R results in decreased food intake and increased energy expenditure by inducing the release of brain-derived

Contract grant sponsor: Ministry of Education, Culture, Sports, Science and Technology of Japan; Contract grant number: 23790654; Contract grant sponsors: Ministry of Health, Labour and Welfare of Japan (for the Third Comprehensive 10-year Strategy for Cancer Control and for Cancer Research); National Cancer Center Research and Development Fund; The Special Grant for young investigators from the President of National Cancer Center

*Correspondence to: Yasuhito Uezono, Division of Cancer Pathophysiology, National Cancer Center Research Institute, 5-1-1, Tsukiji, Chuo-ku, Tokyo 104-0045, Japan. E-mail: yuezono@ncc.go.jp

Received 28 February 2012; Accepted 22 March 2012

DOI 10.1002/syn.21559

Published online 27 March 2012 in Wiley Online Library (wileyonlinelibrary.com).

neurotropic factor (BDNF) in the hypothalamus, which suggests that BDNF is a downstream mediator of MC4R signaling (Xu et al., 2003).

In the present study, we identified changes in the expression of MC3R, MC4R, POMC, and BDNF in the rat hypothalamus in both an early- and late-stage cancer cachexia model. The present findings may provide new insight into the mechanisms that underlie stage-dependent cancer cachexia.

All experiments were conducted in accordance with the ethical guidelines of the International Association for the Study of Pain (Zimmermann, 1983) and approved by the Committee for Ethics of Animal Experimentation of National Cancer Center. Efforts were made to minimize the numbers and any suffering of animals used in the following experiments. The human gastric cancer cell-line 60As6, originating from the human scirrhous gastric cancer cell line HSC60, was established as described previously (Yanagihara et al., 2004). Seven-week-old male F344/N-mu (mu/mu) rats were used. Rats were purchased from CLEA Japan (Tokyo, Japan) and held under standard laboratory conditions (23°C ± 1°C with a 12-h light/dark cycle). Food and water were available ad libitum. Rats were housed singly and, after a 2-week adaptation period, randomly assigned to a tumor or control group. For tumor implantation, rats were anesthetized with isoflurane. Approximately 1 × 10^6 60As6 cells suspended in phosphate-buffered saline (PBS) were then implanted between the peritoneum and the abdominal wall of the central abdomen. Non-tumor controls underwent the same procedure but only received PBS injection. Body weight and food consumption were measured 2, 4, 6, 8, 10, 12, 14, and 16 weeks after tumor implantation. Rats were decapitated at both 8 weeks, as early-stage cancer cachexia, and 16 weeks, as late-stage cancer cachexia. The weights of epididymal fat and the gastrocnemius muscle were measured 8 and 16 weeks after tumor implantation. For real-time reverse transcription PCR, brains were rapidly removed, and the hypothalamic area was dissected on an ice-cold metal plate. Total RNA was isolated from the hypothalamic area using ISOGEN (Niponjine) according to the manufacturer's instructions. First-strand cDNA was reverse transcribed from 5 μg of total RNA by using a SuperScript™ first-strand synthesis system (Invitrogen) in a final volume of 100 μL. Diluted cDNA (2 μL) was amplified in a rapid thermal cycler (LightCycler; Roche Diagnostics) in 10 μL of LightCycler 480 SYBR Green I Master (Roche) and each oligonucleotide. Primer sequences for the genes of interest [MC4R, MC3R, POMC, BDNF, and glyceraldehyde-3-phosphate dehydrogenase (GAPDH)] are shown in Table I. To quantify the PCR products, LightCycler 480 quantification software was used to analyze the exponential phase of amplification and the melting curve, as recommended by the manufacturer. The amount of target mRNA in the experimental group relative to that in the control was determined from the resulting fluorescence and threshold values (C_T) using the $2^{-\Delta\Delta C_T}$ method (Livak and Schmittgen, 2001).

TABLE I. Primer sequences for the rat genes characterized in this experiment

Gene	Primers
GAPDH	Forward primer 5′CCCCCAATGTATCCGTTGTG 3′
	Reverse primer 5′TAGCCCAGGATGCCCTTTAGT 3′
MC4R	Forward primer 5′GCTGCAGGAAGATGAACTCC 3′
	Reverse primer 5′TCCAGAGGTGGAGGGAAGTA 3′
MC3R	Forward primer 5′CCGCCGATAACCATGAACT 3′
	Reverse primer 5′GTTAGGCAGCGTCGGATAAG 3′
POMC	Forward primer 5′TCCTCAGAGAGCTGCCTTTC 3′
	Reverse primer 5′TGTAGCAGAATCTCGGCATCT 3′
BDNF	Forward primer 5′AGCGCGAATGTGTTAGTGGT 3′
	Reverse primer 5′GCAATTGTTTGCCTCTTTTTCT 3′

All data are presented as the mean ± SEM. All the statistical parameters used in the experiments were calculated using GraphPad PRISM. The statistical significance of differences between groups was assessed with Student's *t*-test.

As shown in Figure 1a, tumor-bearing rats showed a significant decrease in body weight from 8 to 16 weeks after the inoculation of tumor cells ($^*P < 0.05$, $^{**}P < 0.01$, and $^{***}P < 0.001$ vs. control group). Consistent with the data, food intake in tumor-bearing rats at 8 and 16 weeks was 11 and 23% lower than that in control rats ($^*P < 0.05$ and $^{**}P < 0.01$ vs. control group; Fig. 1b). At 8 weeks after inoculation, the weight of epididymal fat tissue, but not that of gastrocnemius muscle, was significantly reduced compared to that in control rats ($^*P < 0.05$ vs. control group; Figs. 1c and 1d). A 73% decrease in the weight of epididymal fat tissue and a 31% decrease in the weight of gastrocnemius muscle were observed in tumor-bearing rats 16 weeks after tumor inoculation ($^{***}P < 0.01$ vs. control group; Figs. 1c and 1d). At 8 weeks after inoculation, when rats exhibited slight anorexia and weight loss, the mRNA levels of MC4R, MC3R, and BDNF were significantly decreased in the hypothalamus of tumor-bearing rats compared to those in control rats (8 weeks, $^*P < 0.05$ and $^{***}P < 0.001$ vs. control group; Figs. 2a, 2b, and 2d). In contrast, the expression of these receptors and BDNF was dramatically increased in the hypothalamus of tumor-bearing rats 16 weeks after inoculation, when rats exhibited severe wasting associated with a significant reduction of both adipose tissue and muscle mass (16 weeks, $^{***}P < 0.001$ vs. control group; Figs. 2a, 2b, and 2d). In addition, while the mRNA level of POMC, which encodes α-MSH, in tumor-bearing mice was not different from that in the control at 8 weeks after inoculation, a remarkable decrease in POMC expression was observed in the hypothalamus of tumor-bearing rats

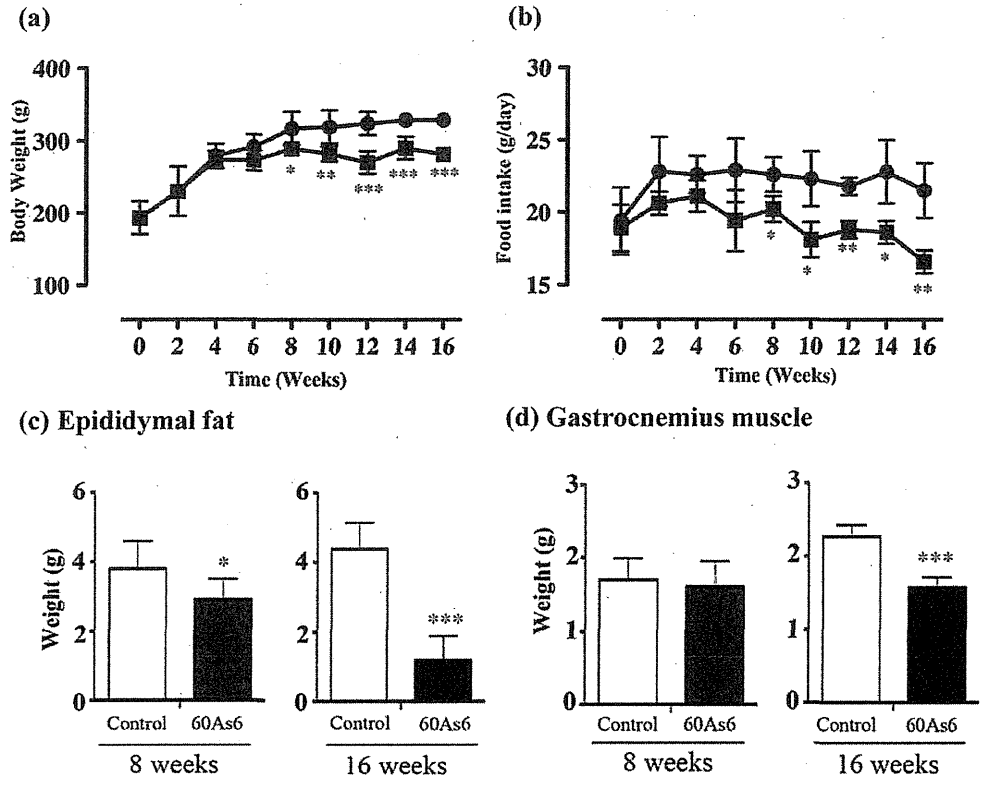

Fig. 1. Body weight and food intake of tumor-inoculated rats. (**a**) Body weight in 60As6 tumor-bearing (■) or PBS-control rats (●). (**b**) Food intake in 60As6 tumor-bearing (■) or PBS-control rats (●). The results represent the mean ± SEM of five to seven rats. $^{*}P < 0.05$, $^{**}P < 0.01$, $^{***}P < 0.001$ versus control group. (**c**) Epididymal fat weight in 60As6 tumor-bearing or PBS-control rats at 8 and 16 weeks after the inoculation of tumor cells. (**d**) Gastrocnemius muscle weight in 60As6 tumor-bearing or PBS-control rats at 8 and 16 weeks after the inoculation of tumor cells. Each column represents the mean ± SEM of five to seven rats. $^{*}P < 0.05$, $^{***}P < 0.001$ versus control group.

16 weeks after inoculation (16 weeks, $^{***}P < 0.001$ vs. control group; Fig. 2c).

The key finding in the present study was that dramatic increases in the expression of both MC3R and MC4R were observed in the hypothalamus of tumor-bearing rats 16 weeks after tumor inoculation, when rats exhibited severe wasting associated with a significant reduction of both adipose tissue and muscle mass, that is, so-called late-stage cachexia. In addition, a remarkable increase in BDNF expression and a decrease in POMC expression in the hypothalamus of tumor-bearing rats were also observed. Central MC3R and MC4R are involved in the regulation of body weight and have been shown under many paradigms to reduce food intake and/or increase energy expenditure (De Jonghe et al., 2011). BDNF in the hypothalamus is thought to regulate the energy balance as a downstream effector of MC4R (Xu et al., 2003). In our preliminary experiments, we found that the locomotor activity of tumor-bearing rats during the dark period was significantly decreased without any changes in the resting energy expenditure, which suggests that the energy expenditure in the dark period was increased in rats with late-stage cachexia (data not shown). Furthermore, MC4R-knockout mice have been shown to exhibit marked hyperphagia and obesity (Huszar et al., 1997), which were blocked by selective MC4R re-expression in the PVN and amygdala (Balthasar et al., 2005). In addition, mice with a double knockout of both MC3R and MC4R exhibit a higher weight gain than those with the deletion of either receptor alone (Chen et al., 2000). Taken together, our present findings raise the possibility that the dramatic up-regulation of MC3R/MC4R signaling, possibly due to the down-regulation of POMC in the hypothalamus, may contribute to the metabolic alterations and reduced availability of nutrients under late-stage cancer cachexia.

At 8 weeks after tumor inoculation, when rats exhibited slight anorexia and weight loss, so-called early-stage cachexia, the expression levels of MC3R, MC4R, and BDNF in the hypothalamus were significantly reduced without any changes in POMC expression. The "adiposity negative-feedback" model of energy homeostasis is based on the premise that circulating signals inform the brain of changes in body

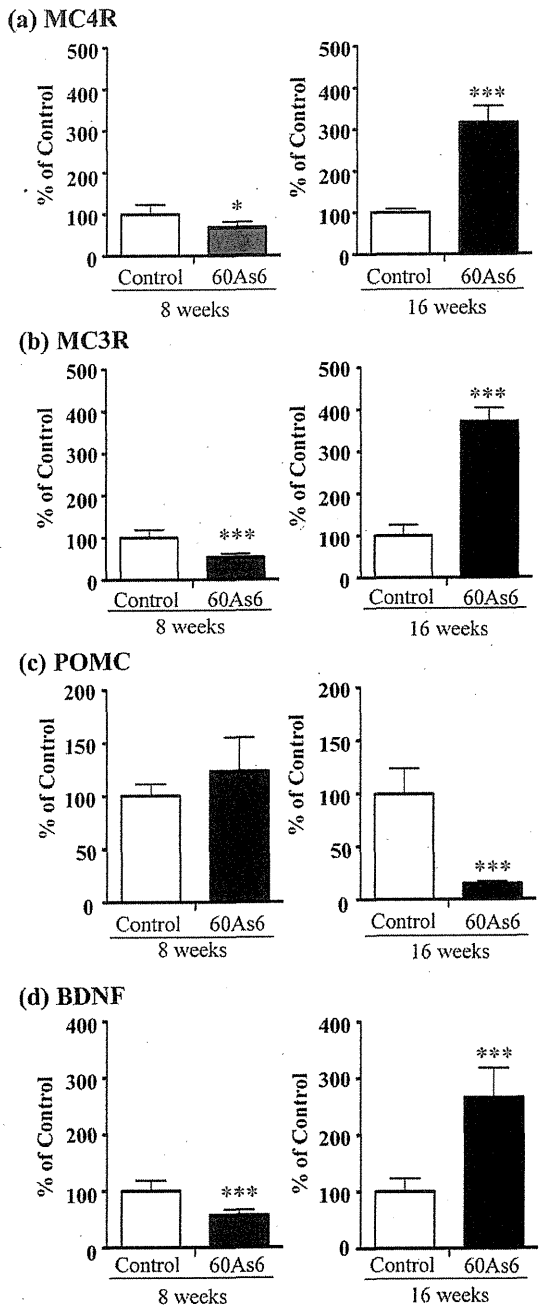

Fig. 2. Transcriptional regulation of MC4R, MC3R, POMC, and BDNF in the hypothalamus induced by tumor inoculation. Expression of MC4R (**a**), MC3R (**b**), POMC (**c**), and BDNF (**d**) in the hypothalamus of tumor-bearing rats on 8 and 16 weeks. The mRNA levels were normalized to those for GAPDH (housekeeping gene), and the results are presented as the mean ± SEM of five to seven mice. $^{*}P < 0.05$, $^{***}P < 0.001$ versus control group.

fat mass and, in response to this input, the brain makes adaptive adjustments to the energy balance to stabilize fat stores (Rousso-Noori et al., 2011). The criteria that have been proposed for a negative-feedback signal include that it circulates at levels proportionate to body fat content and that it promotes weight loss by acting on neuronal systems implicated in energy homeostasis. Many hormones have been implicated in the regulation of central melanocortin signaling, including many nutrients (free fatty acids, glucose), cytokines (interleukin-6, tumor necrosis factor-α), and the adipocyte-secreted hormone leptin (Deboer and Marks, 2006). In the present model, early-stage cachexia model rats exhibited a significant but slight decrease in epididymal fat. Although additional studies will be required to clarify the mechanism of the downregulation of MC3R, MC4R, and BDNF in early-stage cachexia model rats, decreased MC3R/MC4R signaling in the hypothalamus may be responsible for the adiposity negative-feedback signal due to a slight decrease in body fat mass.

In conclusion, our present data provide the first evidence that opposite changes in MC3R/MC4R expression and possible downstream signaling in the hypothalamus occur between the early and late stages in the development of cancer cachexia. Our findings may be important for studying the pathogenesis of stage-dependent cancer cachexia and for the future development of effective treatments for cancer cachexia.

REFERENCES

Acharyya S, Butchbach ME, Sahenk Z, Wang H, Saji M, Carathers M, Ringel MD, Skipworth RJ, Fearon KC, Hollingsworth MA, Muscarella P, Burghes AH, Rafael-Fortney JA, Guttridge DC. 2005. Dystrophin glycoprotein complex dysfunction: A regulatory link between muscular dystrophy and cancer cachexia. Cancer Cell 8:421–432.

Balthasar N, Dalgaard LT, Lee CE, Yu J, Funahashi H, Williams T, Ferreira M, Tang V, McGovern RA, Kenny CD, Christiansen LM, Edelstein E, Choi B, Boss O, Aschkenasi C, Zhang CY, Mountjoy K, Kishi T, Elmquist JK, Lowell BB. 2005. Divergence of melanocortin pathways in the control of food intake and energy expenditure. Cell 123:493–505.

Chen AS, Marsh DJ, Trumbauer ME, Frazier EG, Guan XM, Yu H, Rosenblum CI, Vongs A, Feng Y, Cao L, Metzger JM, Strack AM, Camacho RE, Mellin TN, Nunes CN, Min W, Fisher J, Gopal-Truter S, MacIntyre DE, Chen HY, Van der Ploeg LH. 2000. Inactivation of the mouse melanocortin-3 receptor results in increased fat mass and reduced lean body mass. Nat Genet 26:97–102.

De Jonghe BC, Hayes MR, Bence KK. 2011. Melanocorotin control of energy balance: Evidence from rodent models. Cell Mol Life Sci 68:2569–2588.

Deboer MD, Marks DL. 2006. Cachexia: Lessons from melanocortin antagonism. Trends Endocrinol Metab 17:199–204.

Fearon KC. 2008. Cancer cachexia: Developing multimodal therapy for a multidimensional problem. Eur J Cancer 44:1124–1132.

Garfield AS, Lam DD, Marston OJ, Przydzial MJ, Heisler LK. 2009. Role of central melanocortin pathway in energy homeostasis. Trends Endocrinol Metab 20:203–215.

Huszar D, Lynch CA, Fairchild-Huntress V, Dunmore JH, Fang Q, Berkemeier LR, Gu W, Kesterson RA, Boston BA, Cone RD, Smith FJ, Campfield LA, Burn P, Lee F. 1997. Targeted disruption of the melanocortin-4 receptor results in obesity in mice. Cell 88:131–141.

Livak KJ, Schmittgen TD. 2001. Analysis of relative gene expression data using real-time quantitative PCR and the $2(-\Delta\Delta C_T)$ method. Methods 25:402–408.

Muscaritoli M, Anker SD, Argiles J, Aversa Z, Bauer JM, Biolo G, Boirie Y, Bosaeus I, Cederholm T, Costelli P, Fearon KC, Laviano

A, Maggio M, RossiFanelli F, Schols A, Sieber CC. 2010. Consensus definition of sarcopenia, cachexia and pre-cachexia: Joint document elaborated by Special Interest Groups (SIG) "cachexia-anorexia in chronic wasting diseases" and "nutrition in geriatrics." Clin Nutr 29:154–159.

Norman K, Pichard C, Lochs H, Pirlich M. 2008. Prognostic impact of disease-related malnutrition. Clin Nutr 27:5–15.

Rousso-Noori L, Knobler H, Levy-Apter E, Kuperman Y, Neufeld-Cohen A, Keshet Y, Akepati VR, Klinghoffer RA, Chen A, Elson A. 2011. Protein tyrosine phosphatase epsilon affects body weight by downregulating leptin signaling in a phosphorylation-dependent manner. Cell Metab 13:562–572.

Tisdale M. 2009. Mechanisms of cancer cachexia. Physiol Rev 89:381–410.

Xu B, Goulding EH, Zang K, Cepoi D, Cone RD, Jones KR, Tecott LH, Reichardt LF. 2003. Brain-derived neurotrophic factor regulates energy balance downstream of melanocortin-4 receptor. Nat Neurosci 6:763–742.

Yanagihara K, Tanaka H, Takigahira M, Ino Y, Yamaguchi Y, Toge T, Sugano K, Hirohashi S. 2004. Establishment of two cell lines from human gastric scirrhous carcinoma that possess the potential to metastasize spontaneously in nude mice. Cancer Sci 95:575–582.

Zimmermann M. 1983. Ethical guidelines for investigations of experimental pain in conscious animals. Pain 16:109–110.

SYNAPSE 66:759–769 (2012)

$GABA_B$ Receptors Do Not Internalize After Baclofen Treatment, Possibly Due to a Lack of β-Arrestin Association: Study With a Real-Time Visualizing Assay

YUKA SUDO,[1,2] MINORU HOJO,[3] YUKO ANDO,[3] MASAFUMI TAKADA,[3] HIROAKI MURATA,[3] SHINJI KURATA,[4] NORIYUKI NISHIDA,[1] AND YASUHITO UEZONO[1,2]*

[1]*Department of Cellular and Molecular Biology, Nagasaki University Graduate School of Biomedical Sciences, Nagasaki 852-8523, Japan*

[2]*Division of Cancer Pathophysiology, National Cancer Center Research Institute, Tokyo 104-0045, Japan*

[3]*Department of Anesthesiology, Nagasaki University Graduate School of Biomedical Sciences, Nagasaki 852-8501, Japan*

[4]*Department of Clinical Physiology, Nagasaki University Graduate School of Biomedical Sciences, Nagasaki 852-8588, Japan*

KEY WORDS β-arrestin; $GABA_B$ receptor; internalization; endocytosis; GRK

ABSTRACT The mechanism of agonist-induced $GABA_B$ receptor ($GABA_BR$) internalization is not well understood. To investigate this process, we focused on the interaction of $GABA_BR$ with β-arrestins, which are key proteins in the internalization of most of the G protein-coupled receptors, and the agonist-induced $GABA_BR$ internalization and the interaction of $GABA_BR$ with β-arrestin1 and β-arrestin2 were investigated in real time using $GABA_BR$ and β-arrestins both of which were fluorescent protein-tagged. We then compared these profiles with those of μ-opioid receptors (μOR), well-studied receptors that associate and cointernalize with β-arrestins. When stimulated by the specific $GABA_BR$ agonist baclofen, $GABA_BR$ composed of $GABA_{B1a}R$ ($GB_{1a}R$) and fluorescent protein-tagged $GABA_{B2}R$-Venus (GB_2R-V) formed functional $GABA_BR$; they elicited G protein-activated inwardly rectifying potassium channels as well as nontagged $GABA_BR$. In cells coexpressing $GB_{1a}R$, GB_2R-V, and β-arrestin1-Cerulean (βarr1-C) or β-arrestin2-Cerulean (βarr2-C), real-time imaging studies showed that baclofen treatment neither internalized GB_2R-V nor mobilized βarr1-C or βarr2-C to the cell surface. This happened regardless of the presence of G protein-coupled receptor kinase 4 (GRK4), which forms a complex with $GABA_BR$ and causes $GABA_BR$ desensitization. On the other hand, in cells coexpressing μOR-Venus, GRK2, and βarr1-C or βarr2-C, the μOR molecule formed μOR/βarr1 or μOR/βarr2 complexes on the cell surface, which were then internalized into the cytoplasm in a time-dependent manner. Fluorescence resonance energy transfer assay also indicated scarce association of GB_2R-V and β-arrestins-C with or without the stimulation of baclofen, while robust association of μOR-V with β-arrestins-C was detected after μOR activation. These findings suggest that $GABA_BR$s failure to undergo agonist-induced internalization results in part from its failure to interact with β-arrestins. **Synapse 66:759–769, 2012.**

INTRODUCTION

$GABA_B$ receptors ($GABA_BR$s) play important roles in controlling inhibitory neurotransmission by GABA in the central and peripheral nervous system (Bettler et al., 2004). The receptors belong to the G protein-coupled receptor (GPCR) family and are the first discovered obligatory heterodimer consisting of $GABA_{B1}$ receptor (GB_1R) and $GABA_{B2}$ receptor (GB_2R) (Agnati

Contract grant sponsors: Ministry of Health, Labor, and Welfare, Japan; National Cancer Research and Development Fund; Foundations for Daiichi-Sankyo Co. Ltd.; Showa-Yakuhin Kako, Co. Ltd.; Nippon Shinyaku Co. Ltd.; Asbio Pharma Co. Ltd.; Tsumura Co. Ltd.; and Ministry of Education, Culture, Sports Science, and Technology of Japan

*Correspondence to: Yasuhito Uezono, Division of Cancer Pathophysiology, National Cancer Center Research Institute, Tokyo 104-0045, Japan. E-mail: yuezono@ncc.go.jp

Received 24 February 2012; Accepted 11 April 2012.

DOI 10.1002/syn.21565

Published online 20 April 2012 in Wiley Online Library (wileyonlinelibrary.com).

et al., 2003; Bettler et al., 2004; Gainetdinov et al., 2004; Uezono et al., 2006). This GB_1R/GB_2R heterodimerization is indispensable for the molecule to locate within the plasma membrane (Couve et al., 1998). Additionally, the two molecules have different functions within the dimers: agonists bind only to GB_1R, while GB_2R transduces the signal though the trimeric G proteins (Gα and Gβγ subunits) to downstream molecules (Galvez et al., 2001; Uezono et al., 2006).

Desensitization and subsequent internalization of these receptors by agonist stimulation is important to avoid their overstimulation and to terminate their agonist-induced signaling (Kelly et al., 2008). The initial step in this process is thought to involve phosphorylation of the receptors by G protein-coupled receptor kinases (GRKs) or second-messenger-regulated kinases, such as protein kinase C or A (Kelly et al., 2008). β-arrestins, composed of β-arrestin1 (βarr1) and β-arrestin2 (βarr2), were identified as proteins that have the ability to desensitize GPCR, and further recognized as endocytic adapters and trafficking mediators of a variety of cell-surface receptors, including GPCRs (Shenoy and Lefkowitz, 2011). Once receptors are phosphorylated by several kinases, βarr1 or βarr2 bind to the phosphorylated receptors, forming the receptor/β-arrestin complex, which is then internalized (Gainetdinov et al., 2004).

Phosphorylation of $GABA_BR$ is unique compared with that of common GPCRs such as β-adrenergic receptor and the μ-opioid receptors (μOR). We and others have previously shown that GRK4 and GRK5 but not GRK2, GRK3, or GRK6 are involved in the GABA- or baclofen-mediated $GABA_BR$ desensitization processes (Ando et al., 2011; Kanaide et al., 2007; Perroy et al., 2003). However, the receptors were not phosphorylated by these kinases (Kanaide et al., 2007; Perroy et al., 2003). Accordingly, GRK4 and GRK5 seem to function solely as anchoring proteins, not as kinases (Kanaide et al., 2007; Perroy et al., 2003; Terunuma et al., 2010).

There are contradictory reports regarding agonist-induced $GABA_BR$ internalization, with recent studies demonstrating that $GABA_BR$ is not internalized by agonist stimulation (Fairfax et al., 2004; Grampp et al., 2007; Perroy et al., 2003; Vargas et al., 2008), while earlier studies showed the opposite. In addition, one report has shown that $GABA_BR$ is constitutively internalized and that this process is accelerated by $GABA_BR$-agonist stimulation (Wilkins et al., 2008).

Although β-arrestins are key proteins in most GPCR internalization, baclofen did not recruit β-arrestins to the plasma membrane and failed to form a complex with $GABA_BR$ (Fairfax et al., 2004; Perroy et al., 2003). However, the studies reporting these results were not performed in real time. More recent reports have shown that $GABA_BR$ is constitutively internalized into the cytosol without receptor activation (Grampp et al., 2007; Vargas et al., 2008; Wilkins et al., 2008). Although investigation of activation and inactivation steps of $GABA_BR$ are necessary to understand GABA-induced regulation in the central and peripheral nervous systems, one of the most important receptor-mediated signaling such as interaction of $GABA_BR$ and β-arrestins is not well understood.

In this study, we focused on the interaction of $GABA_BR$ with β-arrestins. We used a real-time analysis with and without stimulation of the agonist. Additionally, we visually analyzed protein-complex formation using fluorescent protein-fused $GABA_BR$ with fluorescent protein-fused β-arrestins in a fluorescence resonance energy transfer (FRET) assay developed by our laboratory (Ando et al., 2011; Kanaide et al., 2007; Uezono et al., 2006). FRET is a useful tool to quantify molecular dynamics in biophysics and biochemistry, such as protein–protein interactions and protein conformational changes (Miyawaki and Tsien, 2000). We compared results from real-time visualization and FRET efficiency of fluorescent protein-tagged $GABA_BR$ complexed to β-arrestins with corresponding results from fluorescent protein-tagged μOR combined to β-arrestins. μOR is well known to interact with β-arrestins and consequently be internalized (Gainetdinov et al., 2004; Groer et al., 2011). This analysis showed that $GABA_BR$ did not associate with β-arrestin, regardless of agonist stimulation.

MATERIALS AND METHODS

Drugs and chemicals

Baclofen was purchased from Tocris Cookson (Bristol, UK). DAMGO ([D-Ala^2, N-MePhe^4, Gly-ol]-enkephalin) was purchased from Sigma (St. Louis, MO). All other chemicals used were of analytical grade and were obtained from Nacalai Tesque (Kyoto, Japan).

Construction of cDNAs

Human $GB_{1a}R$ and GB_2R clones were generously provided by Dr. N.J. Fraser (Glaxo Wellcome, Stevenage, UK). Cerulean, a brighter variant of cyan fluorescent protein (Rizzo et al., 2004) was provided by Dr. D.W. Piston (Vanderbilt University, Nashville, TN), and Venus, a brighter variant of yellow fluorescent protein (Nagai et al., 2002), was provided by Dr. T. Nagai (Hokkaido Univ., Sapporo, Japan). Human GRK4 was provided by Dr. A. De Blasi (Neuromed, IRCCS, Pozzilli, Italy); bovine GRK2 were provided by Dr. J.L. Benovic (Thomas Jefferson University, Philadelphia, PA). Rat βarr1 and βarr2 were provided by Dr. Nagayama (Nagasaki Univ., Nagasaki, Japan). Rat μOR was provided by Dr. N. Dascal (Tel Aviv Univ., Tel Aviv, Israel). Venus-fused $GABA_BR$ and μOR, and Cerulean-fused βarr1 and βarr2 were created by ligating their cDNA sequences into the *Not*I I sites of the corresponding Venus or Cerulean sites, as reported previously (Ando

et al., 2011; Kanaide et al., 2007; Uezono et al., 2006). All cDNAs for transfection into cells were subcloned into pcDNA3.1 (Invitrogen, San Diego, CA).

Cell culture and transfection

BHK cells were grown in Dulbecco's modified eagle medium supplemented with 10% fetal bovine serum, penicillin (100 U/ml), and streptomycin (100 μg/ml) at 37°C and 5% CO_2. For transfection experiments, BHK cells were seeded at a density of 1–2 × 10^5 cells/35-mm in glass-bottomed culture dishes (World Precision Instrument, Sarasota, FL) for 24 h. Transient transfection was then performed with Hilymax transfection reagent (Dojindo, Kumamoto, Japan) using a total of 0.6 μg cDNA, according to the manufacturer's protocol. Cells were analyzed under confocal microscopy 24 h after transfection.

Real-time monitoring of the mobilization of receptors and β-arrestins fused to fluorescence proteins

We constructed fluorescent-protein-fused GB_2R-V, μOR-V, βarr1-C, and βarr2-C molecules to visually monitor mobilization of receptors and β-arrestins. BHK cells that coexpressed GB_2R-V with βarr1-C or βarr2-C were treated with baclofen for the indicated periods, then placed in 4-(2-hydroxyethyl)-1-piperazineethanesulfonic acid (HEPES)-buffered saline. Translocation or complex formation of GB_{B2}R-V and βarr-C was observed for 120 min. Cells coexpressing μOR-V and βarr1-C or βarr2-C were treated with the μOR agonist DAMGO in the same manner. For visualization, a 63× magnification and 1.25 numerical aperture oil immersion objective with pinhole was used. Both, Cerulean and Venus were excited by a 458-nm laser, and images were obtained by placing the dish onto a stage in a Zeiss LSM510 META confocal microscope (Carl Zeiss, Jena, Germany), as described previously (Kanaide et al., 2007; Uezono et al., 2006).

Confocal microscopy for FRET analysis

For the analysis of protein-complex formation of GB_2R-V and μOR-V with β-arr1-C or β-arr2-C, we used the FRET assay. GB_{1a}R or GB_2R-V was coexpressed with either β-arr1-C or β-arr2-C in BHK cells. These BHK cells were cultured in 35-mm glass-bottomed dishes and cotransfected with each of DNA. Both, Cerulean and Venus were excited by a 458-nm laser, and images were obtained by placing the dish onto a stage in a Zeiss LSM510 META confocal microscope.

Photobleaching and calculation of FRET efficiency

To confirm FRET to find association of Cerulean- and Venus-fused proteins, we monitored acceptor photobleaching analysis in BHK cells that coexpressed GB_{1a}R, GB_2R-V, βarr2-C, and GRK4, or cells that coexpressed μOR-V, βarr2-C, and GRK2. FRET was measured by imaging Cerulean before and after photobleaching Venus with 100% intensity from a 514-nm argon laser for 1 min, a duration that efficiently bleached Venus with little effect on Cerulean. An increase of donor fluorescence (Cerulean) was interpreted as evidence of FRET from Cerulean to Venus. All experiments were analyzed from at least six cells with three independent regions from their plasma membranes. As a control, we examined the FRET efficiency of the unbleached area of plasma membranes from at least three areas in the same cell. In some cases, we performed the photobleaching assay using BHK cells coexpressing Venus + Cerulean, or GB1aR-C + GB2R-V + βarr2 +GRK4 as negative and positive controls of FRET, respectively. The photobleaching assay was performed as previously described (Kanaide et al., 2007).

FRET efficiency was calculated using emission spectra before and after acceptor photobleaching of Venus (Miyawaki and Tsien, 2000). According to this procedure, if FRET is occurring, then photobleaching of the acceptor (Venus) should yield a significant increase in fluorescence of the donor (Cerulean). Increase of donor spectra due to desensitized acceptor was measured by the Cerulean emission (at 488 nm) from spectra before and after acceptor photobleaching. FRET efficiency was then calculated using the equation $E = 1 - I_{DA}/I_D$, where I_{DA} is the peak of donor (Cerulean) emission in the presence of the acceptor, and I_D is the peak in the presence of the sensitized acceptor, as previously described (Riven et al., 2003). Before and after this bleaching, Cerulean images were collected to assess changes in donor fluorescence.

Statistical analysis

Data are expressed as mean ± SEM. Differences between two groups were examined for statistical significance using paired t test. GraphPad Prism software (San Diego, CA) was used to analyze data for statistical significance and to fit curves. For comparisons between multiple groups, one-way analysis of variance was used, followed by Scheffe's test. A P value of less than 0.05 was classified as statistically significant.

RESULTS

Fluorescence-tagged $GABA_B$R activation of GIRK channels

In this study, we used fluorescence protein-tagged $GABA_B$R instead of wild type $GABA_B$R. This is because, as we previously showed, fluorescence-tagged GB_{1a}R-Venus or GB_2R-Venus behave like non-tagged, wild type $GABA_B$R. That is, they display G

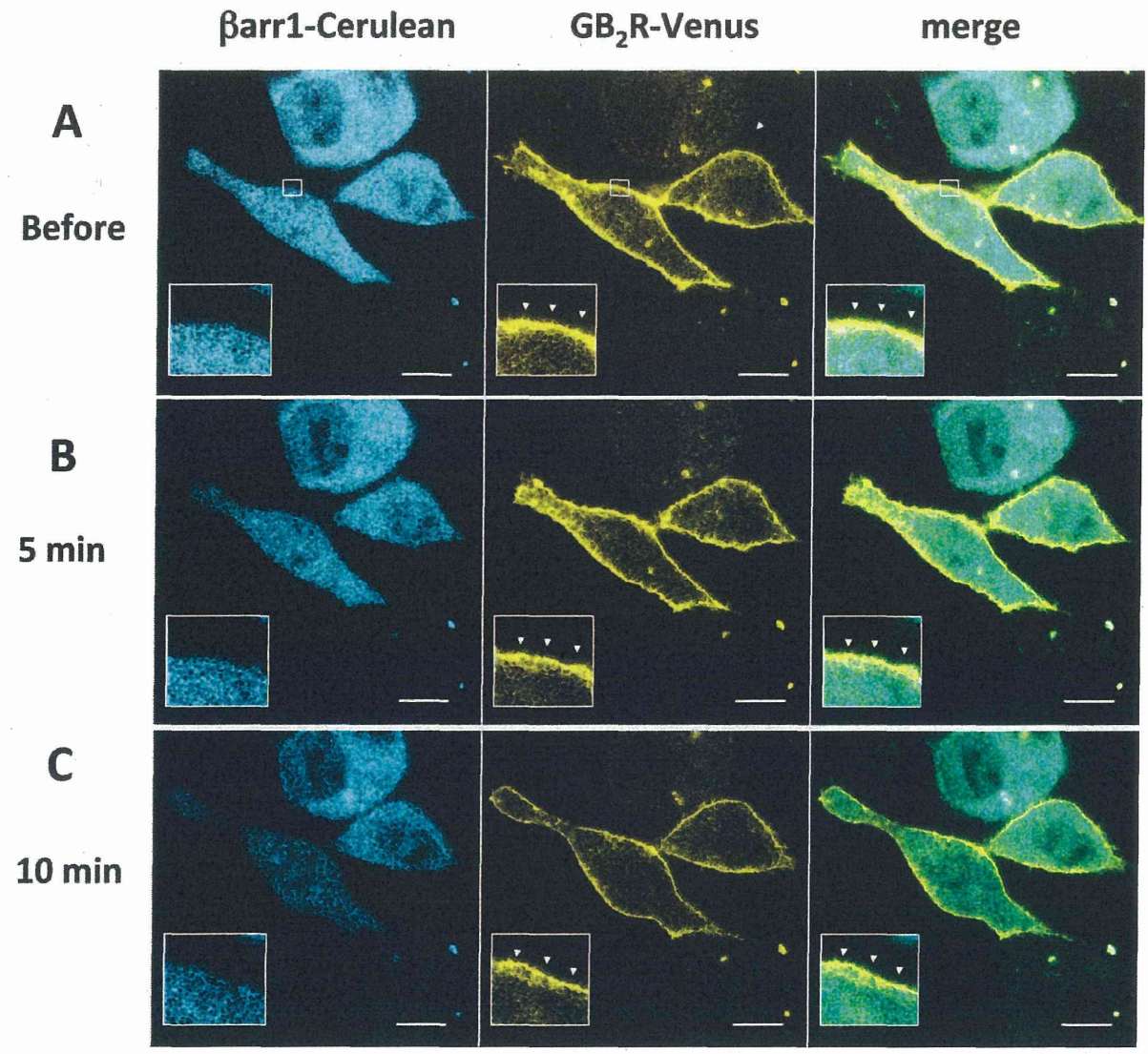

Fig. 1. Confocal imaging of the translocation of GB_2R-V and βarr2-C in BHK cells expressing $GB_{1a}R$, GB_2R-V, βarr2-C, and GRK4. Visualization of GB_2R-V and βarr2-C in BHK cells before (**A**), and 5 min (**B**) and 10 min (**C**) after stimulation with 10^{-4} M baclofen. Arrowheads show GB_2R-V on the plasma membranes. Similar results were obtained in at least six independent experiments. Calibration bar = 10 μm.

protein-activated inwardly rectifying potassium-channel activation, channels known to be activated by $GABA_BR$ stimulation (Ando et al., 2011; Kanaide et al., 2007; Uezono et al., 1998, 2006).

Activation of $GABA_BR$ did not induce receptor internalization

We first determined the distribution and translocation of functional $GABA_BR$ and β-arrestins in BHK cells and examined whether β-arrestins were able to associate with $GABA_BR$ in response to receptor stimulation. In living BHK cells, coexpressing $GB_{1a}R/GB_2R$-V and GRK4 with βarr1-C or βarr2-C, both βarr1 and βarr2 proteins were diffusely distributed in the cytosol (Figs. 1 and 2). GB_2R-V was expressed exclusively on the plasma membrane (Figs. 1 and 2). Although expression of $GB_{1a}R$ on the plasma membrane was not found, our previous reports showed that $GB_{1a}R$ and GB_2R formed heterodimers on the plasma membranes during the same experimental procedure (Uezono et al., 2006). In this study, when cells expressing $GB_{1a}R/GB_2R$-V, βarr2-C, and GRK4 received baclofen at 10^{-4} M for 5 min or GABA at 10^{-4} M for 5 min (data not shown), both agonists failed to mobilize βarr1-C from the cytosol to plasma

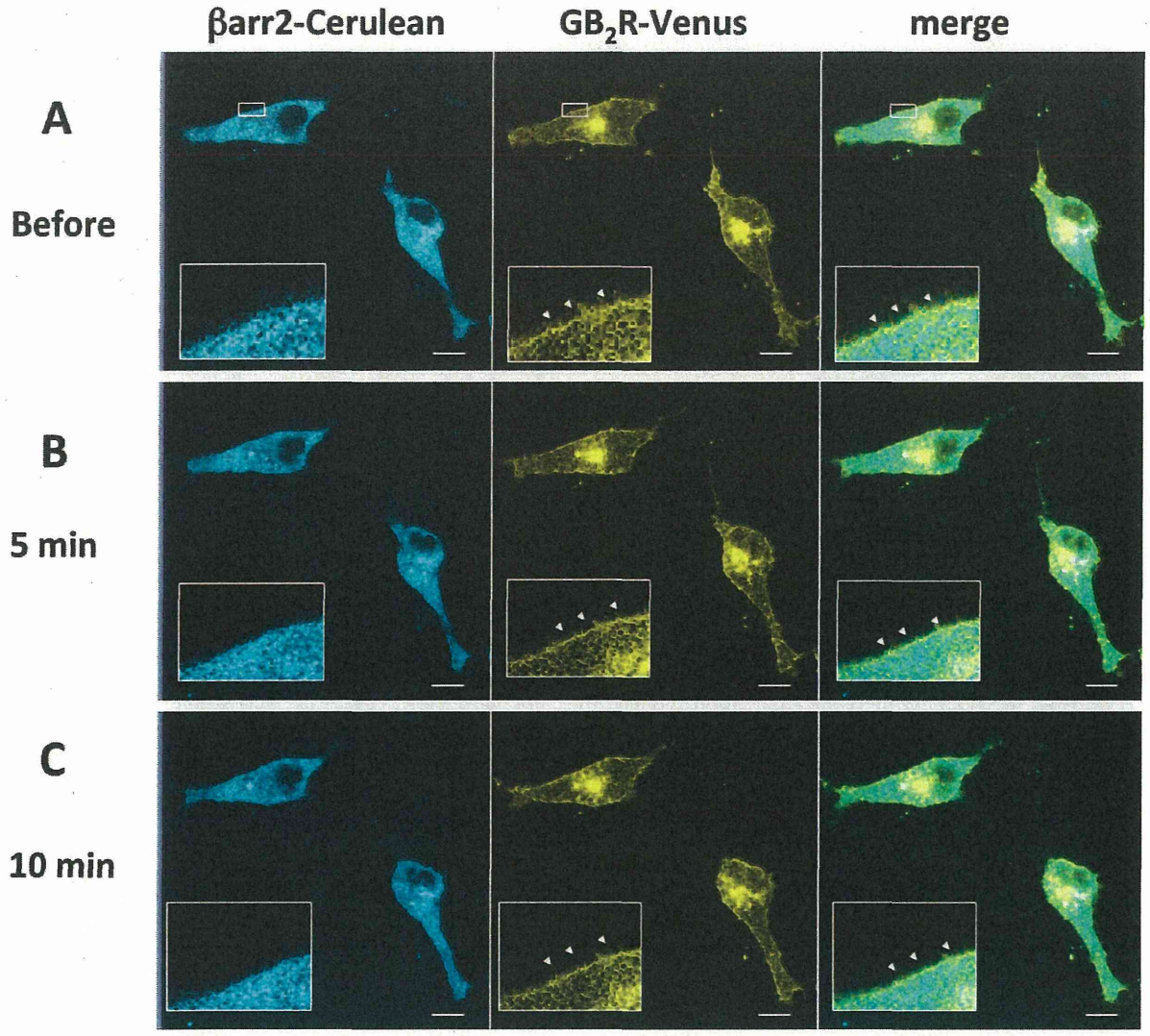

Fig. 2. Confocal imaging of the translocation of GB_2R-V and βarr1-C in BHK cells expressing $GB_{1a}R$, GB_2R-V, βarr1-C, and GRK4. Visualization of the GB_2R-V and βarr1-C in BHK cells before (**A**), and 5 min (**B**) and 10 min (**C**) after stimulation with 10^{-4}M baclofen. Arrowheads show GB_2R-V on the plasma membranes. Similar results were obtained in at least six independent experiments. Calibration bar = 10 μm.

membranes (Fig. 1) for up to 120 min (data not shown). The concentration of baclofen and GABA and duration chosen were those causing submaximal cellular responses and the translocation of GRK4 to the plasma membrane, with subsequent formation of the GB_2R/GRK4 complex that would desensitize $GABA_BR$ (Ando et al., 2011; Kanaide et al., 2007; Uezono et al., 1998, 2006). Similar results were observed in cells coexpressing βarr2-C instead of βarr1-C (Fig. 2).

For the real-time critical measurement of the intensity of GB_2R-V combined with βarr2-C or βarr1-C, we calculated the intensity strength within the cytosolic area, shown as the red line in Figure 3A. Results showed that, when activated by baclofen at 10^{-4} M, intensities of both GB_2R-V and βarr2-C gradually decreased. This was possibly due to quenching by exposure to laser power (Fig. 3). As shown in Figure 3C, there were almost no changes, for up to 120 min, in the intensities of GB_2R-V and βarr2-C after stimulation by baclofen (data not shown), indicating no internalization of GB_2R-V into the cytosol and no movement of βarr2-C at any time examined. Similar results were observed in cells expressing GB_2R-V with βarr1-C (Fig. 3D). We also examined constitutive internalization of GB_2R in BHK cells coexpressing $GB_{1a}R$/GB_2R-V, βarr2-C, and GRK4; for up to 120 min, we were unable to detect any internalization profiles of GB_2R-V or any mobilization of βarr2-C (data not shown).

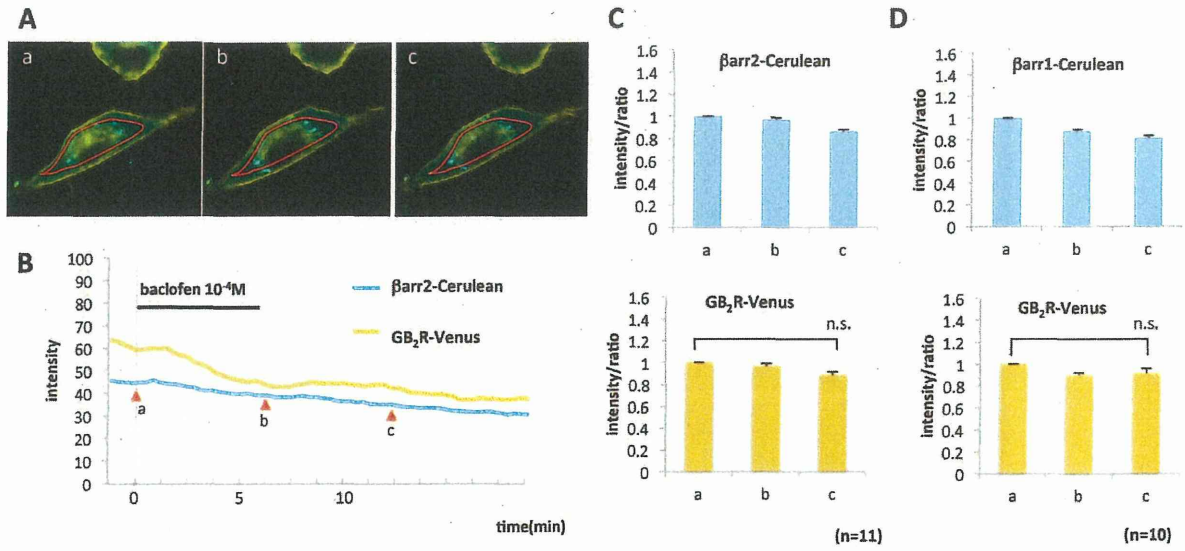

Fig. 3. Time courses of changes in intensities of GB_2R-V, βarr2-C, or βarr1-C in BHK cells. **A**: Confocal imaging of the BHK cells expressing $GB_{1a}R$, GB_2R-V, βarr2-C, and GRK4. For calculation, intensities of the areas within the red line (cytosol) were measured. **B**: Changes in intensities before (a), and 5 min (b) and 10 min (c) after stimulation of baclofen (10^{-4} M) in real time. **C**: Intensity ratio of βarr2-C and GB_2R-V at the indicated points as in (B). **D**: Intensity ratio of βarr1-C and GB_2R-V at the indicated points as in (B). Data were expressed as intensity ratio of the level at "b" or "c"/the level at "a."

We then investigated μOR internalization induced by the μOR agonist DAMGO. In cells expressing μOR-V, GRK2, and βarr1-C or βarr2-C, we applied DAMGO at 10^{-7} M for 5 min, the concentration and duration that cause submaximal μOR activation and receptor desensitization. This resulted in dramatic translocation of βarr1-C and βarr2-C into the plasma membranes and subsequent internalization with μOR-V (Figs. 4 and 5). In the same cells, βarr1-C or βarr2-C were translocated and concentrated into dot-like shapes on the plasma membranes for the first 4–5 min stimulation by DAMGO, as indicated by arrowheads. Consequently, βarr1-C or βarr2-C was eventually internalized into the cytosol (Figs. 4 and 5).

DAMGO-induced βarr1-C or βarr2-C internalization and translocation into the cells were also measured, as shown in Figure 6. The intensity of μOR-V was increased by application of DAMGO, and small granules were observed, shown within the area of the red line (Fig. 6A). In addition, corresponding decreases of βarr2-C intensity were also detected. As shown in Figures 6B and 6C, increases in the intensities of μOR-V and decreases in βarr2-C were detected in a time-dependent manner (Figs. 6B and 6C). Similar results were observed in cells expressing μOR-V, GRK2, and βarr1-C instead of βarr2-C (Fig. 6D).

FRET and acceptor photobleaching analysis of BHK cells coexpressing $GB_{1a}R$ and GB_2R-V with βarr2-C

Because βarr1-C or βarr2-C was translocated into the plasma membranes following μOR activation, but not following $GABA_BR$ activation, we used FRET analysis to determine whether βarr2-C interacts and forms a protein complex with GB_2R. We used BHK cells that coexpressed $GB_{1a}R$, $GB_{B2}R$-V, βarr2-C, and GRK4 or cells that coexpressed μOR-V, βarr2-C, and GRK2.

In such cells, photobleaching analysis of baclofen-stimulated cells demonstrated that FRET efficiency at the cell membranes was not remarkably changed at 5 min after stimulation with baclofen at 10^{-4} M (Fig. 7A). FRET efficiency before stimulation, and 1, 2, 5, 10, 30, and 60 min (and 120 min, data not shown) after stimulation was not significantly changed (Fig. 7B). Similar results were obtained when we used βarr1-C instead of βarr2-C (data not shown). In contrast, photobleaching analysis of DAMGO-stimulated BHK cells demonstrated that FRET efficiency was increased 1 min after stimulation and reached maximal value at 5 min, then gradually decreased for 30 min (Fig. 7B), demonstrating that the receptor/β-arrestin complex was formed by stimulation of the agonist.

DISCUSSION

Recent study has shown that DAMGO activation of μOR recruited both βarr1 and βarr2 to the μOR then cause robust internalization in mouse embryonic fibroblasts (mef; Groer et al., 2011). They showed no internalization profiles of μOR by DAMGO in mef derived from βarr1/βarr2 knockout mice. Furthermore, βarr1 or βarr2 reintroduction into these mef